Interpolation-Based Reconstructions for Raster-Scanned Backscatter X-ray Radiography

Junho Lee [a], Jinwoo Kim [b], Seungjun Yoo [a], Ho Kyung Kim [a,b,*]
[a] *School of Mechanical Engineering, Pusan National Univ., Busandaehakro 63beon-gil, Busan 46241*
[b] *Center for Advanced Medical Engineering, Pusan National Univ., Busandaehakro 63beon-gil, Busan 46241*
[*] *Corresponding author: hokyung@pusan.ac.kr*

1. Introduction

Screening cargo containers at ports and vehicles at borders has been essential for homeland security [1]. Imaging techniques are the most popular for screening. While the scanning radiography using a deep-penetrating megavoltage x-ray beam is typical [2], this method suffers from low contrast of low-Z materials, which are the basis of explosives and drugs, because the contrast is proportional to the target thickness multiplied by the difference of linear attenuation coefficients between the target and its neighbors [3]. Instead, the backscatter imaging using a kilovoltage x-ray spectrum (e.g. 220 kV) provides higher contrast for low-Z materials because the contrast is proportional to the difference of the Compton coefficients relative to the background coefficient [3]. This backscatter radiography has been successfully applied to industry [4], including cargo-container and vehicle inspection [5,6].

The backscatter x-ray imaging also requires a scanning system; the x-ray beam irradiates the vehicle vertically using a collimator wheel while the vehicle moves horizontally. For each spotting of the x-ray beam, the large-area detector placed behind the x-ray source measures the backscattered x-ray photons, which constitutes a single-pixel signal in the resulting 2D image. Therefore, this raster scanning approach cannot avoid geometric distortion in images [7]. The distortion will be more severe with the mismatch between the angular velocity of the wheel and the vehicle speed. We develop backscatter image reconstruction methods to compensate for the geometric artifacts based on interpolation.

2. Methods

2.1 Raster-Scan Sampling

As shown in Fig. 1, the one-sided backscatter x-ray imaging is similar to the raster scanning: the circular pattern (due to the circular shape of the collimator aperture) of image capture and reconstruction. The slope of the raster-scan line is mainly determined by the angular velocity ω of the collimator wheel and the vehicle speed v_x. Assuming that the sampling period is based on the detector readout time Δt, the scan line is not straight but follows a tangential function.

Figure 2(a) shows the scan lines with respect to various ω 's relative to $\omega_0 = 1$ for a fixed v_x . p represents the scan-line period for $\omega_0 = 1$. Figure 2 shows the sampling pitch in the vertical direction relative to the equi-distant sampling ($\Delta y = 1$). The sampling pitch

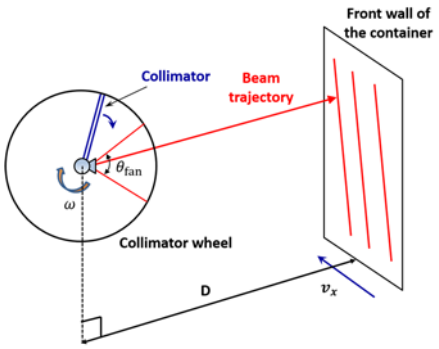

Fig. 1. Sketch describing the raster scanning of a vehicle using a collimator wheel. For the backscatter x-ray imaging, a large-area detector is placed behind the x-ray source.

is not a constant size. For a single raster-scan line, the sampling pitch decreases rapidly, approaches the minimum value, and then increases reversely. From these results, it is expected that the raster scanning will result in distortions in the reconstructed images.

2.2 Raster-Scan Reconstructions

In this study, we propose two interpolation methods for the raster-scan reconstructions: (1) the bilinear interpolation and (2) the distance-weighted interpolation. For a rectangular grid point (x_i, y_i), in the reconstruction image domain, the bilinear-interpolation method first takes four surrounding scan data: $I(m; l_n)$, $I(m+1; l_n)$, $I(m; l_{n+1})$, and $I(m+1; l_{n+1})$, where $I(m; l_n)$ represents the detector signal obtained for the m th sampling along the n th scan line. These data points correspond to the apexes of a parallelogram, which includes (x_i, y_i) inside. Then, we determine $I(x_i, y_i)$ from the bilinear interpolation.

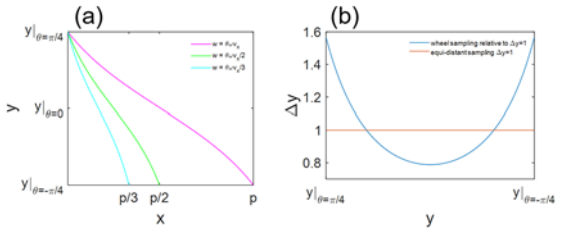

Fig. 2. (a) Raster scan lines with respect to various angular velocities of the collimator wheel relative to a given vehicle speed. (b) Sampling pitch in the vertical direction relative to the equi-distant sampling.

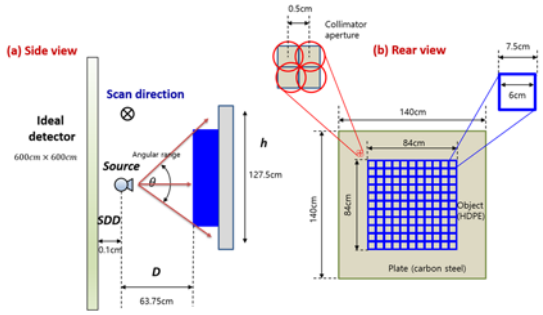

Fig. 3. The Monte Carlo geometry mimicking the backscatter x-ray imaging system. A mesh-shaped plastic is used as an object to be scanned.

On the other hand, the distance-weighted interpolation is the average of four apex points weighted by the distances between (x_i, y_i) and the apexes.

2.3 Monte Carlo Simulations

To mimic the backscatter x-ray imaging, we performed Monte Carlo (MC) simulations using a commercial MC radiation transport code (MCNP, RSICC, Oak Ridge, TN). The object to be scanned was a rectangular grid mesh made of a high-density polyethylene. A large-area detector was placed behind the x-ray source. Detailed MC geometry, including dimensions, is shown in Fig. 3.

3. Preliminary Results

For the equi-distantly sampled (Δy = constant) Shepp-Logan phantom along the raster-scan lines, Fig. 4 shows the performance of the distance-weighted interpolation for reconstruction in comparison with the conventional raster-scanning method. Three different raster scanning situations were considered: $p = \frac{v_x}{\omega} = 1$, 2, and 3. While

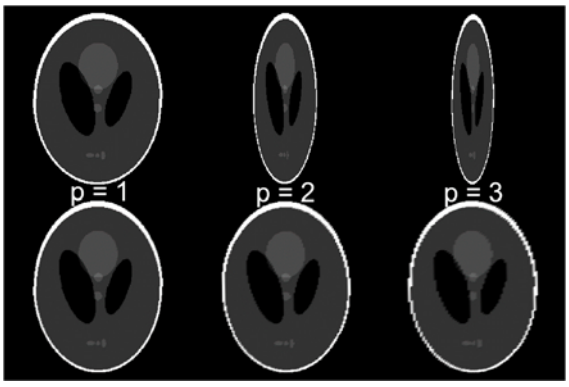

Fig. 4. Comparison of raster-scan reconstructions for equi-distant sampling of the Shepp-Logan phantom. Upper row images result from the simple raster scanning for p = 1, 2, and 3 (correspondingly, $\omega = v_x$, $v_x/2$, and $v_x/3$). Lower row images show the corresponding images reconstructed by the distance-weighted interpolation method.

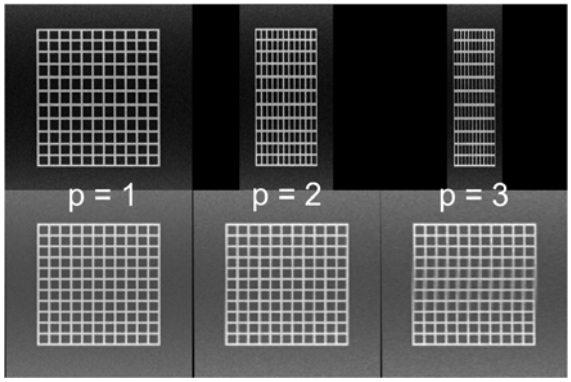

Fig. 5. Comparison of reconstructed backscatter x-ray radiography images for the Monte Carlo simulation data. Upper row images result from the simple raster scanning for p = 1, 2, and 3 (correspondingly, $\omega = v_x$, $v_x/2$, and $v_x/3$). Lower row images show the corresponding images reconstructed by the bilinear-interpolation method.

the conventional method results in shrunken images with increasing p, as expected, the reconstruction with distance-weighted interpolation restores the original image.

For the backscatter signals obtained from the Monte Carlo simulations, the raster scanning was also performed for three different situations, as shown in Fig. 5. Similarly, the conventional raster scanning results in distorted images. Even if $\omega = v_x$ or p = 1, the mesh size is non-uniform along the vertical direction, as expected from Fig. 2(b). On the contrary, the proposed bilinear interpolation method reconstructs well the mesh phantom, except for $p = 3$ case, which is an extreme case. We have observed the similar results with the distance-weighted interpolation.

4. Conclusions

We have shown that the conventional raster scanning for backscatter x-ray radiography resulted in large distortions in reconstructed images, depending on the mismatch between the angular velocity of the collimator wheel and the vehicle speed, using the MC simulations. Even for the matched case, the raster scanning showed non-uniformity along the vertical direction. We have developed the raster-scan reconstruction algorithms based on interpolation, and the performance was excellent. Even for the extreme raster-scanning condition (three times larger vehicle speed than the wheel angular velocity), the proposed method restored reasonably the original image with some distortions around the relatively fine-sampling regions. More quantitative evaluations of the developed methods will be presented at the conference.

ACKNOWLEDGEMENTS

This work was conducted as a part of the research projects of “Development of automatic screening and

hybrid detection system for hazardous material detecting in port container" financially (20200611) supported by the Ministry of Oceans and Fisheries, Korea.

REFERENCES

[1] G. Zentai, X-Ray Imaging for Homeland Security, International Journal of Signal and Imaging Systems Engineering, Vol. 3, pp. 13-20, 2010.
[2] H. E. Martz, Jr., S. M. Glenn, J. A. Smith, C. J. Divin, and S. G. Azevedo, Poly- versus Mono-Energetic Dual-Spectrum Non-Intrusive Inspection of Cargo Containers, IEEE Transactions on Nuclear Science, Vol. 64, pp. 1709-1718, 2017.
[3] G. Harding, H. Strecker, and R. Tischler, X-Ray Imaging with Compton-Scatter Radiation, Philips Technical Review, Vol. 41, pp. 46-59, 1983.
[4] E. M. A. Hussein and E. J. Waller, Review of One-Sided Approaches to Radiographic Imaging for Detection of Explosives and Narcotics, Radiation Measurements, Vol. 29, pp. 581-591, 1998.
[5] R. D. Swift, Mobile X-Ray Backscatter Imaging System for Inspection of Vehicles, Proc. SPIE, Vol. 2936, pp. 124-132, 1997.
[6] J. Callerame, X-Ray Backscatter Imaging: Photography through Barriers, Powder Diffraction, Vol. 21, pp. 132-135, 2006.
[7] D. B. Plewes and E. Vogelstein, Exposure Artifacts in Raster Scanned Equalization Radiography, Medical Physics, Vol. 11, pp. 158-165, 1984.